Nox1-derived oxidative stress as a common pathogenic link between obesity and hyperoxaluria-related kidney injury

J. Sáenz-Medina, M. Muñoz, A. Sanchez, C. Rodriguez, E. Jorge, C. Corbacho, D. Izquierdo, M. Santos, E. Donoso, E. Virumbrales, et al.

Urolithiasis

ISSN 2194-7228

Urolithiasis
DOI 10.1007/s00240-019-01170-w

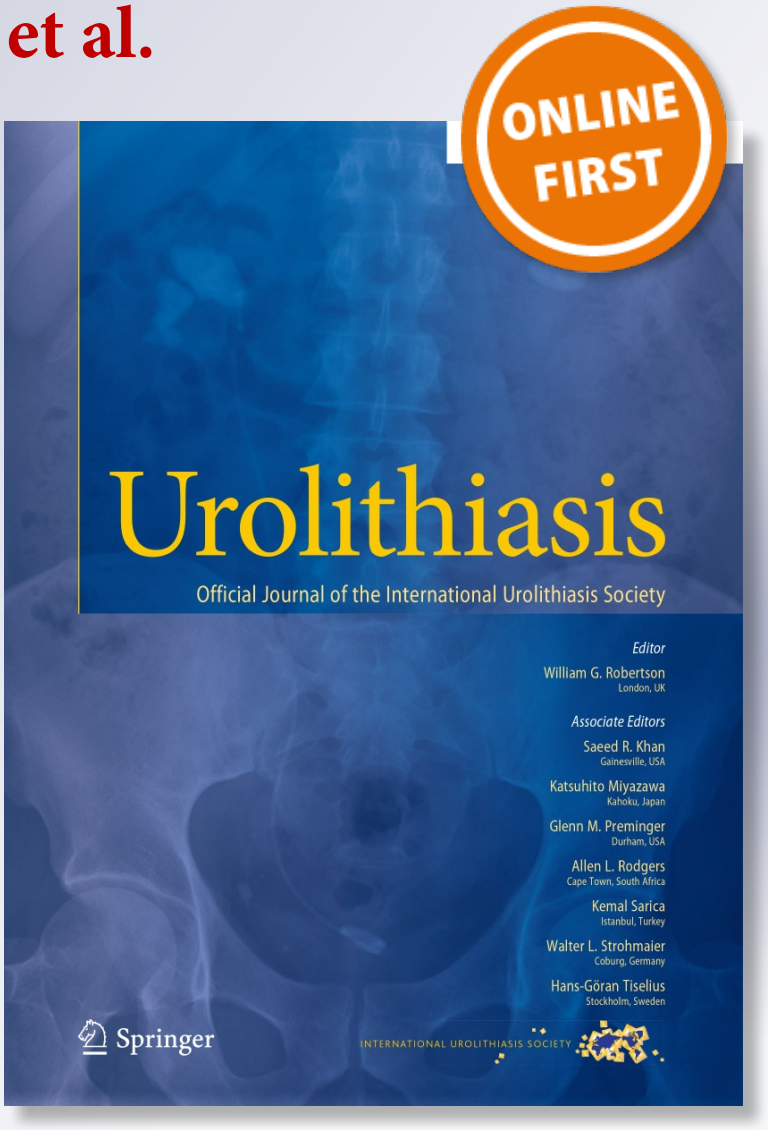

Springer

Urolithiasis
https://doi.org/10.1007/s00240-019-01170-w

ORIGINAL PAPER

Nox1-derived oxidative stress as a common pathogenic link between obesity and hyperoxaluria-related kidney injury

J. Sáenz-Medina[1] · M. Muñoz[2] · A. Sanchez[2] · C. Rodriguez[2] · E. Jorge[3] · C. Corbacho[4] · D. Izquierdo[4] · M. Santos[5] · E. Donoso[3] · E. Virumbrales[3] · A. Sanchez[6] · E. Ramil[7] · M. J. Coronado[8] · D. Prieto[2] · J. Carballido[9]

Received: 21 June 2019 / Accepted: 25 October 2019

Abstract

Specific relationships among reactive oxygen species, activation pathways, and inflammatory mechanisms involved in kidney injury were assessed in a combined model of obesity and hyperoxaluria. Male Wistar rats were divided into four groups: Control, HFD (high fat diet), OX (0.75% ethylene glycol), and HFD + OX (combined model) Changes in basal O_2^- levels were evaluated by chemiluminescence in renal interlobar arteries and renal cortex. Furthermore, the effect of different inhibitors on NADPH-stimulated O_2^- generation was assessed in renal cortex. Oxidative stress sources, and local inflammatory mediators, were also determined, in parallel, by RT-PCR, and correlated with measures of renal function, urinary biochemistry, and renal structure. Rats from the HFD group developed overweight without lipid profile alteration. Tubular deposits of crystals were seen in OX and severely enhanced in HFD + OX groups along with a significantly higher impairment of renal function. Basal oxidative stress was increased in renal cortex of OX rats and in renal arteries of HFD rats, while animals from the combined HFD + OX group exhibited the highest levels of oxidative stress in renal cortex, derived from xanthine oxidase and COX-2. NADPH oxidase-dependent O_2^- generation was elevated in renal cortex of the OX group and markedly enhanced in the HFD + OX rats, and associated to an up-regulation of Nox1 and a down-regulation of Nox4 expression. High levels of oxidative stress in the kidney, of OX and HFD + OX groups were also associated to an inflammatory response mediated by an elevation of TNFα, COX-2, NFκB1 MCP-1, and OPN. Oxidative stress is a key pathogenic factor in renal disease associated to hyperoxaluria and a common link underlying the exacerbated inflammatory response and kidney injury found under conditions of both obesity and hyperoxaluria. Nox1 pathway must be considered as a potential therapeutic target.

Keywords Obesity · Oxidative stress · Urolithiasis · NADPH oxidase · Renal injury

Abbreviations

CaOx	Calcium oxalate
COX	Cyclooxygenase
CRD	Chronic renal disease
EG	Ethylene glycol
HFD	High fat diet

Electronic supplementary material The online version of this article (https://doi.org/10.1007/s00240-019-01170-w) contains supplementary material, which is available to authorized users.

D. Prieto and J. Carballido authors equally contributed to this work.

✉ J. Sáenz-Medina
javiersaenzmedina@yahoo.es

[1] Department of Urology, Hospital Universitario Puerta de Hierro-Majadahonda, Universidad Rey Juan Carlos, Calle Manuel de Falla, 1, Majadahonda, 28222 Madrid, Spain

[2] Department of Physiology, Facultad de Farmacia, Universidad Complutense de Madrid, Madrid, Spain

[3] Department of Clinical Biochemistry, Hospital Universitario Puerta de Hierro-Majadahonda, Madrid, Spain

[4] Department of Pathology, Hospital Universitario Puerta de Hierro-Majadahonda, Madrid, Spain

[5] Medical and Surgical Research Facility, Instituto de Investigación Sanitaria Puerta de Hierro, Madrid, Spain

[6] Biobank, Instituto de Investigación Sanitaria Puerta de Hierro, Madrid, Spain

[7] Molecular Biology and DNA Sequencing Facility, Instituto de Investigación Sanitaria Puerta de Hierro, Madrid, Spain

[8] Confocal Microscopy Facility, Instituto de Investigación Sanitaria Puerta de Hierro, Madrid, Spain

[9] Department of Urology, Hospital Universitario Puerta de Hierro-Majadahonda, Universidad Autónoma de Madrid, Madrid, Spain

Published online: 05 November 2019

MCP	Monocyte chemoattractant protein
NADPH	Nicotinamide adenine dinucleotide phosphate
NF-κB	Nuclear factor kappa-light-chain-enhancer of activated B cells
NO	Nitric oxide
Nox	NADPH oxidase enzymes
O_2^-	Superoxide
OPN	Osteopontin
ROS	Reactive oxygen species

Introduction

The incidence of kidney stones in industrialized countries is increasing from approximately 3% in the 70 s to a current prevalence of around 9%. It continues to be an important factor of chronic kidney disease (CKD) leading to chronic tubular nephritis, which is involved in 15–20% of end-stage CKD. Dietary factors, obesity, and diabetes are strongly associated with a history of kidney stones and may be responsible of the increasing prevalence of urolithiasis [1].

Epithelial damage as a key factor of stone formation has been associated with the production of reactive oxygen species (ROS). Elevation of *N*-acetyl beta glucosaminidase, alpha glutathione transferase, thiobarbituric acid reactive substances, and malondialdehide urinary levels of lithiasic patients suggests the involvement of ROS-associated inflammatory mechanisms in the production of calcium oxalate (CaOx) stones [2]. It has also been suggested the involvement of ROS-associated inflammatory mechanisms in the production of human calcium oxalate (CaOx) crystals [2].

High levels of ROS, after exceeding the antioxidant defense systems, oxidize various molecules such as DNA, proteins, carbohydrates or lipids, a phenomenon known as oxidative stress (OS). In mammalian cells, ROS production sources include the mitochondrial respiratory chain, the xanthine oxidase enzyme, the NADPH oxidases (**Nox**s), the uncoupled nitric oxide synthase (NOS) and other hemoproteins [3]. Recent studies demonstrate that NADPH inhibition reduces local renal inflammation and tubular deposition of CaOx crystals in rat models of hyperoxaluria [4, 5].

Obesity is major risk factor for CKD independent of the other comorbidities such as diabetes and dyslipidemia [6]. As a target organ of lipotoxicity, the kidney exhibits glomerulopathy as well as lesions in the proximal tubule. The mitochondrial metabolism accumulation of intracellular fatty acids in obesity produces lipid metabolites such as ceramide or diacylglycerol. Thus, generation of intracellular ROS damages cell organelles, alters intracellular signal mechanisms, releases pro-inflammatory factors, and produces lipid-induced apoptosis [7]. On the other hand, oxidative stress and increased NADPH oxidase-derived ROS generation have been associated with the inflammatory response and kidney injury associated with hyperoxaluria [8]. Furthermore, we have recently demonstrated that metabolic syndrome aggravates morphological alterations and renal function impairment in rats with hyperoxaluria [9].

The aim of this study was to assess the effects of oxidative stress on renal structure and function, in a combined rat model of hyperoxaluria and obesity, induced with high fat diet (HFD) to explain the greater amelioration of the renal function in lithiasic patients where obesity, as an inflammatory state, is present.

Materials and methods

Animal model

All animal care and experimental protocols conformed to the European Union Guidelines for the Care and the Use of Laboratory Animals (European Union Directive 2010/63/EU) and were approved by the Institutional Animal Care and Use Committee of Puerta de Hierro Hospital Health Research Institute.

Twenty male wistar rats, 28 days old, were housed in standard conditions and received either standard chow (9% fat, 58% carbohydrates and 33% protein), or 60% high fat diet (HFD) (D12492; Research Diets, containing on caloric basis 60% fat, 20% carbohydrate and 20% protein), and water ad libitum, during 8 weeks.

In the last 3 weeks, drinking water was substituted by 0.75% ethylene glycol (EG) in five animals of each group, as an established animal model of kidney stone formation, triggered by hyperoxaluria. Therefore, four groups of five animals were established: control, HFD, OX (EG 0.75%), and HFD + OX. Rats were euthanized at 12 weeks of age by slow release of CO_2 in a methacrylate box and subsequent exsanguination for blood samples. The kidneys were quickly removed and placed either in cold physiological saline solution or in 10% formaldehyde.

Plasma and urinary biochemistry

Fasting blood and urine were collected after 24 h in a metabolic cage, immediately before the sacrifice. Serum glucose, cholesterol, triglycerides, uric acid, and creatinine were measured with the spectrophotometer ADVIA Chemistry Analyzer multi Siemens 2400 which quantifies the parameters after a series of enzymatic reactions.

24 h urine samples were analyzed for pH, citrate, oxalate, and creatinine. Creatinine clearance (CrCl) was calculated from the following equation: CrCl (mL/min) = [urine creatinine (mg/dL) * urine volume (mL/24 h)]/[serum creatinine (mg/dL) * 1440 (min)].

Measurement of superoxide production by chemiluminescence

Changes in basal O_2^- levels were measured in renal cortex and in interlobar arteries, by lucigenin-enhanced chemiluminescence, as previous described [10]. Furthermore, NADPH was added to cortex samples to assess it as enzymatic source of ROS. Samples were equilibrated in PSS for 30 min at room temperature and then incubated in the absence and the presence of different ROS inhibitors allopurinol (100 µM) and NS398 (1 µM) and the selective Nox1/Nox4 inhibitor GKT137831 (0.3 µM) for 30 min at 37 °C. Posteriorly, specimens were transferred to microliter plate containing 5 µM bis-*N*-methylacridium nitrate (lucigenin) in the absence and presence of different ROS sources and of stimulation with NADPH which was added previous to determination. Chemiluminescence was measured in a luminometer (BMG Fluostar Optima), and for calculation, baseline values were subtracted from the counting values under the different experimental conditions and O_2^- production was normalized to dry tissue weight.

Renal histology and immunofluorescence staining

Kidney samples were immersion fixed in 10% phosphate-buffered formalin in 0.1 M sodium phosphate buffer (PB), cryoprotected in 30% sucrose in PB and snap frozen in liquid nitrogen and stored at − 80 °C. Sections (4 µm thickness) were stained with hematoxylin and eosin (HE) to count crystal deposits. Most representative fields at × 100 magnification were assessed in each section, with the observer, a specialized urology pathologist, blinded to the animal groups. Crystal deposits (% in total tubules) and interstitial inflammation (% of animals affected) were counted.

Immunofluorescence staining was performed to detect expression of COX-1, Nox1, TNFα, and OPN on sections of renal cortex fixed in paraformaldehyde. Target enzymes expression were determined by immunofluorescence by incubating renal sections from Wistar rats with polyclonal primary antibodies: anti-Nox1, (ab55831), anti-COX2, (ab 15191), anti-TNFα, (Ab 34674), and anti-Osteopontin (Ab 69498) from Abcam, Cambridge, UK, for 24 h at 4 °C. Samples were then incubated with Alexa Fluor 488 (Invitrogen) secondary antibody. Nuclei were stained with To-PRO(T-3605, Thermo,-Fisher). Sections were mounted with PBS/Glycerol. Slides stained only with the secondary antibody were used as negative controls to ensure that the secondary antibody does not unspecifically bind to certain cellular components. Images of the specimens were collected with a TCS SP5 confocal microscope (Leica Microsystems, Wetzlar, Germany).

Quantitative RT-PCR

Renal cortex samples were preserved in RNA—later at 4 °C during 1 day and frozen at – 80 ℃ until RNA purification. After thawing, tissues were resuspended in Trizol and homogenized by the MagNA Lyser System (Roche). Total RNA was isolated by RNeasy kit (QIAGEN) including on-column DNAse Digestion, following manufacture Protocol. The preparations obtained had adequate spectrophotometric quality for our purposes.

RNA concentration was determined by spectrophotometry and 500 ng of each sample were reverse transcripted to cDNA using the "First-Strand cDNA Synthesisprotocol (NZYtech)". Relative quantification of gene expression in relation to the level of the reference GAPDH gene was performed in an LC480 (Roche). The target genes were analyzed using Real Time Ready Single Assays (Roche), designed for *Ratus norvegicus*: SPP1 (coding for rat osteopontin, Assay ID: 504587), Ccl2 (coding for rat MCP-1, Assay ID: 500760), Nox1 (Assay ID: 506243), Nox4 (Assay ID: 500694), COX-2 (Assay ID: 502964), and NF-KB (Assay ID: 500911). Target gene used was GAPDH (Assay ID: 503799).

To avoid any residual genomic DNA, Ccl2, NF-kB, Nox4, SPP1, and GAPDH assays included one intron-spanning region. For Nox-1, TNF-alpha, and COX-2, we added total RNA of all the samples, ensuring a minimum difference of ten cycles between the cDNA amplification and RNA amplification.

Statistical analysis

For O_2^- measurements, results are expressed as counts per minute (cpm) per mg of tissue in renal cortex samples and arterial segments, respectively, as means (SEM) of five animals.

The statistical differences between means of four groups of animals were compared using the ANOVA or Kruskal–Wallis test, and *t* student or U-Mann–Whitney tests for two groups comparisons. Categorical variables (Inflammatory infiltration) were analyzed with Chi-square test. Data are expressed by mean and SEM and percentage and standard error in case of categorical variables, establishing a level of statistical significance of 95%. GraphPad was used for the statistical analysis of the results.

Results

Obesity and hyperoxaluria model establishment and kidney function description

Under fasting conditions, rats fed a HFD for 8 weeks exhibited overweight compared to control group. They did not

display significant dyslipidemia or hyperglycemia, although HFD group showed a trend for higher blood glucose and triglycerides, and lower HDL cholesterol levels (Suppl. Table 1).

Hyperoxaluria and lithiasis model establishment was demonstrated by increased oxaluria and crystal tubular deposits in the OX and HFD + OX groups. Crystal deposits were significantly higher in the HFD + OX group (54% vs 14%, $p < 0.001$). Likewise, interstitial inflammation was uniformly present in each animal of the HFD + OX group, but only in one out of five animals of the OX group. (Table 1, Fig. 1).

Impairment of renal function was observed in the OX group and aggravated in HFD + OX rats, as shown by the progressive deterioration of creatinine clearance values (Table 1). 24 h urinary levels of citrate were lower in HFD group, in contrast with rats fed with normal chow (Table 1).

Oxidative stress is associated with kidney injury and exacerbated when obesity and hyperoxaluria converge

To assess the role of oxidative stress in the kidney injury above reported, lucigenin-enhanced chemiluminescence was performed to measure O_2^- levels in samples of kidney cortex and renal interlobar arteries. Basal O_2^- levels were higher in renal cortex and arteries of the OX and the HFD groups, respectively, compared to controls. Interestingly, cortex samples of the HFD + OX group exhibited even higher O_2^- levels than those of the OX group (Fig. 2).

Xanthine oxidase and COX-2 pathways were evaluated by examining the effects of the COX-2 inhibitor NS-398 and the xanthine oxidase inhibitor allopurinol on renal cortex basal O_2^- levels. RT-PCR for COX-2 was also carried out in all groups. Allopurinol inhibited higher basal O_2^- levels observed in cortex from the OX group, although differences were not reached. In the HFD + OX group, both inhibitors reduced enhanced ROS generation (Fig. 3).

RT-PCR COX-2 expression levels were higher in OX and HFD + OX groups, although statistical differences were not reached (Fig. 4a). Nevertheless, immunofluorescence staining showed an enhanced COX-2 expression in the renal cortex of the HFD, OX and HFD + OX groups, compared to controls (Fig. 4b). These findings suggest the influence of COX-2 in oxidative stress-mediated injury. In the same way, changes in the lowering effect assessed by allopurinol in groups OX and HFD + OX, suggest xanthine oxidase implication as other source of oxidative stress and inflammation.

Role of NADPH oxidase and Nox1 and Nox4 isoforms as sources of renal oxidative stress

To assess the enzymatic sources of ROS, changes in NADPH-stimulated ROS generation was measured by chemiluminescence in samples of renal cortex. Involvement of Nox1 and Nox4 isoforms was further assessed by the addition of the selective Nox1/Nox4 inhibitor GKT137831, and RT-PCR.

NADPH-dependent O_2^- levels were significantly higher in the OX group compared to controls and these values further increased nearly by twofold over the OX group values in the HFD + OX group (Fig. 5a). Treatment with GKT137831

Table 1 Renal function and kidney morphological changes after 8 weeks of HFD versus control rats on standard chow and 0.75% ethylene glycol as the drinking water in the last 3 weeks (OX)

Renal function	Control	HFD	OX	HFD + OX	*p*
Diuresis (cc)	44 (4.5)	29.2 (5.3)	35.8 (8.9)	14.9 (2.1)	0.02
Creatinine (mg/dl)	0.38 (0.02)	0.36 (0.07)	0.58 (0.1)	1.31 (0.7)	NS
Creatinine clearance (ml/min)	2.02 (0.26)	1.90 (0.27)	1.31 (0.12)	0.82 (0.25)	0.02
Morphological changes					
Kidney tubular crystal deposits (% of tubular involvement)	0 (0)	0(0)	14.4 (3.9)	54 (9.9)	0.001
Interstitial inflammation (% of animals affected)	0 (0)	0 (0)	20 (20)	100 (0)	0.01
Urinary Biochemical					
pH	6.9 (0.18)	7 (0.16)	7.8 (0.34)	7 (0.16)	0.039
Oxaluria (mg/24 h)	0.37 (0.04)	0.29 (0.04)	8.78 (1.26)	4.26 (0.97)	< 0.001
Citraturia (mg/24 h)	7.04 (2.58)	1.78 (0.42)	3.37 (1.29)	1.10 (0.18)	0.047

Data are expressed as mean (SEM) except for interstitial inflammation, which is a proportion. Significant differences were analyzed by ANOVA test, except for creatinine in which distribution does not follow the normal distribution (KS < 0.05), and Chi square in case interstitial inflammation

HFD high fat diet

NS: $p > 0.05$. OX, EG 0.75% in drinking water during 3 weeks. Measures were determined in five rats of each group

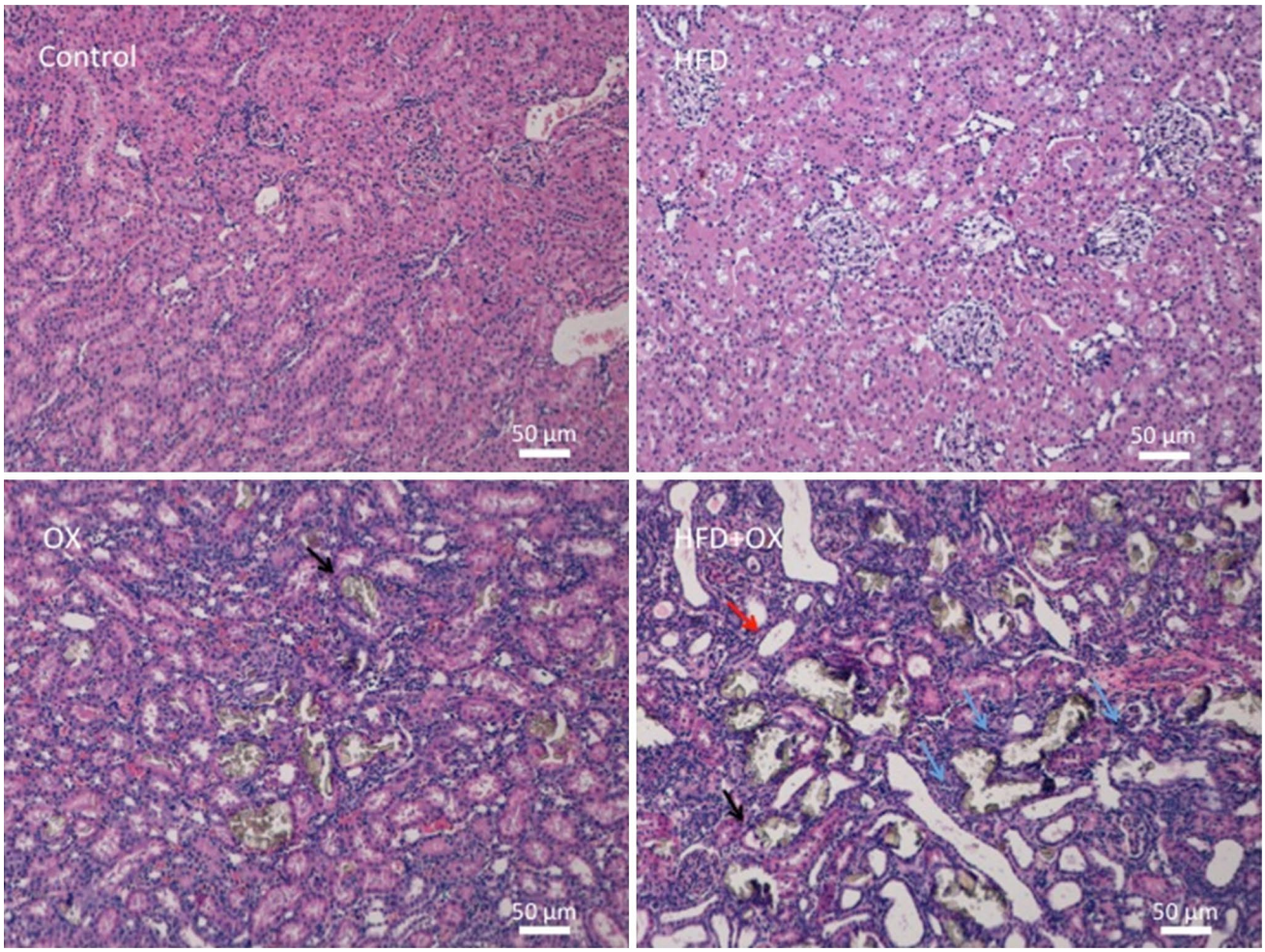

Fig. 1 Renal cortex 10×hematoxylin–eosin comparative light microscopy images in which renal atrophy (red arrow), crystal tubular deposits (black arrows), and interstitial mononuclear infiltrates (blue arrow) can be seen, in OX group, but above all, in HFD + OX group, in a parallel form as is described in Table 1

inhibited NADPH-derived oxidative stress in all four groups (Fig. 5b). These results suggest that NADPH oxidase largely contributes to oxidative stress which probably underlies the greatest tubular injury and renal damage seen in the HFD + OX group.

Interestingly, differential patterns of Nox subunits gene expression were found among the various experimental groups with up-regulation of Nox1 and down-regulation of Nox4 (Fig. 6a, b). Thus, levels of Nox1 mRNA were higher in OX and HFD + OX groups compared to controls, and showed a marked threefold increase over the OX group in HFD + OX rats (Fig. 6a). Nox1 immunofluorescence staining labeled vascular tissue (glomeruli), tubules, and interstitium (Fig. 6c). Nox4 gene expression showed an opposite pattern, being less expressed as injury was higher (Fig. 4b). These findings suggest the influence of Nox1 in triggering an important oxidative stress response, which is enhanced when obesity and hyperoxaluria come together and probably underlies kidney injury.

Local inflammatory response (TNF α, NFκB1, OPN y MCP-1)

Local inflammatory kidney response was further evaluated in kidney cortex samples by assessing RT-PCR expression of TNF α and MCP-1, as cytokines involved in the inflammatory response, NFκB1, as redox-sensitive oxidative stress induced transcription factor, and OPN, as a tubular marker of CaOx nephrolithiasis.

A positive correlation between augmented oxidative stress and the pro-inflammatory NFκB1 pathway was found, as both NFκB1 and TNFα gene expression were significantly enhanced in the OX and HFD + OX groups compared to controls. Moreover, immunofluorescence showed a slight

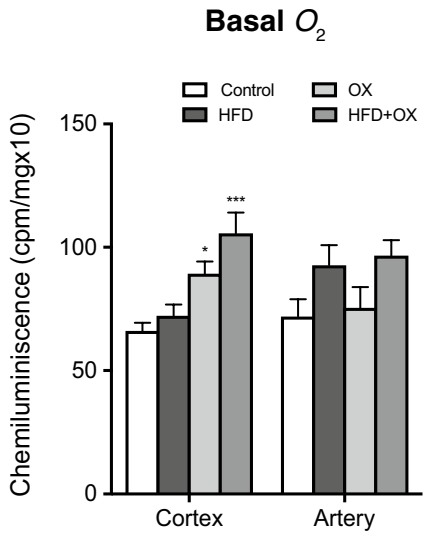

Fig. 2 Comparative levels of basal ROS generation in kidney cortex and renal interlobar arteries measured by lucenin-enhanced chemiluminescence. Renal artery O_2^- levels were higher in the HFD-fed groups, while higher cortex O_2^- levels were generated in the 0.75% ethylene glycol-treated groups. Highest O_2^- production was observed both in artery and cortex when both circumstances converged. Results are expressed as counts per minute (cpm) per mg of tissue. Bars represented mean ± SEM of five animals. Statistical differences were calculated with ANOVA and *t* test $*p < 0.05$ versus basal levels, $***p < 0.001$ versus basal levels

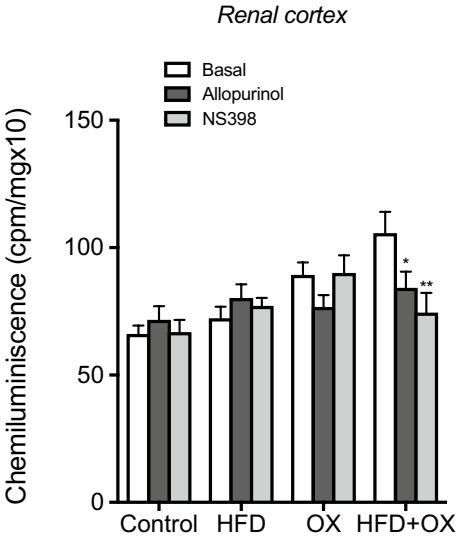

Fig. 3 Allopurinol reduces basal O_2^- production in kidney cortex tissue from 0.75% ethylene glycol-treated rats, while both COX-2 and xanthine oxidase inhibition reduces basal oxidative stress in renal cortex from the HFD and OX group. Effects of allopurinol (xanthine oxidase inhibitor) and NS-398 (COX-2 inhibitor) on basal production of O_2^- levels in renal cortex. Comparative analysis between control group, HFD-fed rats, 0.75% ethylene-treated rats and combined model. Results are expressed as counts per minute (cpm) per mg of tissue. Bars represented mean ± SEM of five animals. Statistical differences were calculated with *t* test $*p < 0.05$ versus basal levels, $**p < 0.01$ versus basal levels

TNFα expression in renal tubules of the HFD group, and an intense labeling of vascular tissue (glomeruli), tubules, and interstitium in the OX and HFD + OX groups (Fig. 7c). These findings suggest the involvement of a renal inflammatory response triggered by oxidative stress in the OX group and exacerbated in the HFD + OX group, in parallel with the renal function impairment observed in OX and aggravated in HFD + OX rats.

On the other hand, the inflammatory local marker MCP-1 was also up-regulated and MCP-1-RNAm levels were markedly increased in the OX and exacerbated in the HFD + OX groups (Fig. 8a), which suggests that tubular damage, secondary to the crystal tubular deposits, was more severe in HFD + OX. OPN gene expression showed the same pattern as MCP-1 in response to hyperoxaluria and CaOx nephrolithiasis induction, being highly expressed in OX and even more in HFD + OX group (Fig. 8b). Immunofluorescence labeling with OPN antibodies, marked predominantly the epithelial layer of tubules of OX kidney cortex samples, and more intensely HFD + OX samples (Fig. 8c).

Discussion

Obesity and metabolic syndrome have been identified as risk factors for the development of nephrolithiasis and loss of renal function associated with urolithiasis, and oxidative stress has been proposed as the common link of the major pathogenic pathways for developing both diabetic nephropathy and urolithiasis. The present study was designed to establish the specific relationships among oxidative stress, obesity, urolithiasis, and renal function to define the specific role of ROS in the worsening of renal function in obese patients with urolithiasis.

Our data first demonstrate that hyperoxaluria induces Nox1-derived ROS generation in the kidney and obesity augments this oxidative stress response and the associated inflammation, thus worsening renal injury and function.

Basal O_2^- levels, measured in renal cortex, were found to be higher in OX and further increased in the HFD + OX group, while basal oxidative stress was enhanced in renal arteries of HFD-fed rats. In vitro and in vivo studies have earlier reported the generation of ROS secondary to the exposition to high levels of oxalate and CaOx crystals, resulting in renal epithelium injury [11]. Moreover, oxidative stress levels have been found to be high in renal arteries and cortex of obese Zucker rats, worsened by HFD, and associated with renal injury and enhanced expression of inflammatory markers [12]. Interestingly, in the present study, the combination of obesity and hyperoxaluria had a synergistic effect on kidney oxidative stress, and greatly enhanced ROS generation in renal cortex, which correlated with an exacerbated inflammatory response, a greater amount of crystal

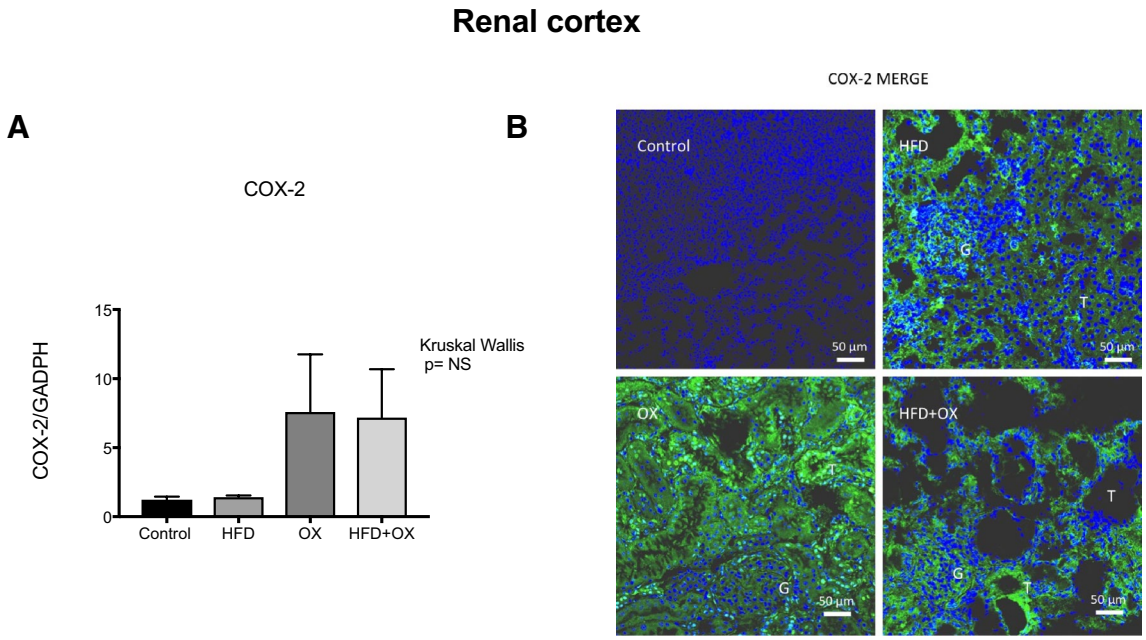

Fig. 4 COX-2 expression is higher, as renal damage is more severe both in glomeruli and in tubules from rat kidney. **a** RT-PCR analysis of COX-2 expression in samples of renal cortex, showing that COX-2 RNAm levels were higher in the OX and HFD + OX groups. Results were quantified by relative quantification of gene expression using COX-2 as the target genes, and GAPDH as reference gene. Results are presented as a ratio of COX-2 expression vs. GADPH from the sample. Data are shown as mean ± SEM of five animals. Significant differences were analyzed using Kruskal–Wallis test $*p < 0.05$, $**p < 0.01$. **b** Immunofluorescence demonstration of COX-2 in renal cortex from rat kidney. Immunofluorescence double labeling for TO-PRO marker (blue areas) demonstrates nuclear staining and for COX-2 protein (green areas), which was distributed throughout the cortex, both in tubules (T) and glomeruli (G). Likewise RT-PCR COX-2 protein expression, was higher in HFD group, OX group and HFD + OX group, when renal damage was more severe. Control group did not show any expression. Scale bars indicate 50 µm. Sections are representative of $n = 3$ animals

deposits with interstitial inflammation and a worsening of the renal function loss.

COX-2 has been implicated in the renal inflammatory response in diabetes and obesity-associated nephropathy [13, 14]. In the present study, COX-2 inhibition reversed the higher cortex basal O_2^- levels observed in HFD + OX group. COX-2 gene expression was increased in both the OX and HFD + OX groups, being highly expressed in tubules, interstitium, and glomeruli. The present findings support previous studies demonstrating that COX-2 is main source of vascular oxidative stress and renal endothelial damage in obesity [13] and further show a COX-2 involvement associated to oxidative stress and renal impairment in lithiasis similar to the functional impairment of murine models of obesity, hypertension or diabetes [15].

Despite uric acid metabolism is certainly a risk factor for stones and is also implicated in cardiovascular and metabolic disease, xanthine oxidase, as hypoxanthine oxidation catalyst, is a critical source of ROS that contributes to endothelial dysfunction and vascular inflammation [16]. Our results showed the implication of xanthine oxidase in ROS synthesis of groups OX and HFD + OX, where the xanthine oxidase inhibitor allopurinol was able to lower basal O_2^- cortex levels. These findings are experimentally supported by other studies in which has been demonstrated the protective role of allopurinol over ROS generation [17].

Mitochondrion and NADPH oxidase have been confirmed as the two major sources of oxidative stress both in obesity-related nephropathy and in oxalate toxicity [18]. In our study, hyperoxaluric rats displayed a significant elevation of NADPH-dependent oxidative stress in renal cortex. Interestingly, NADPH-dependent cortical O_2^- levels increased almost by twofold in hyperoxaluric rats fed a HFD. In all cases, NADPH-dependent augmented ROS generation was inhibited by the selective Nox1/Nox4 inhibitor GKT 137831. In agreement with these data, cortex Nox1 gene expression was found to follow a parallel pattern of augmented O_2^- generation, showing higher levels in the

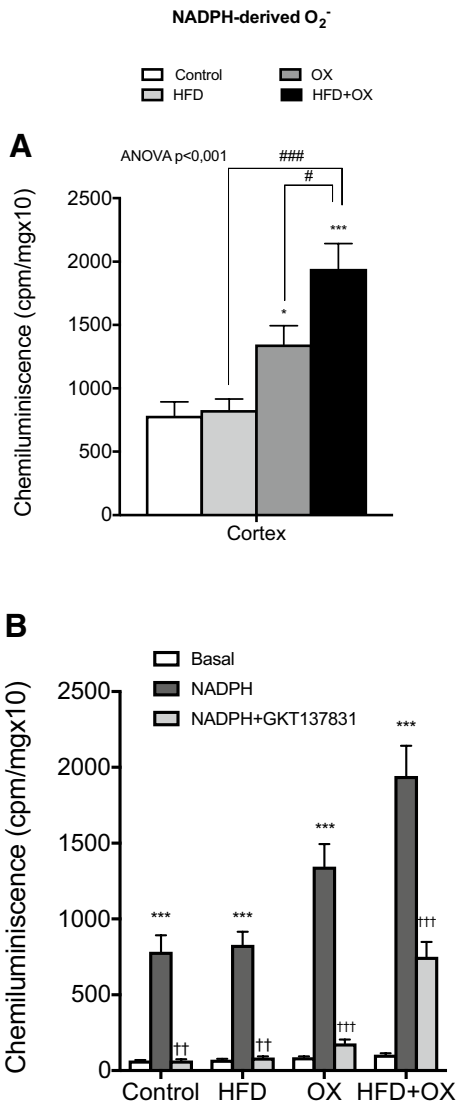

Fig. 5 NADPH oxidase-induced ROS generation is higher in cortex samples of the OX group, exacerbated in the HFD + OX group and inhibited by the selective Nox1/4 inhibitor GKT137831. **a** NADPH-stimulated O_2^- generation in renal cortex, measured by lucigenin-enhanced chemiluminescence. Comparative analysis between control group, HFD fed rats, 0.75% ethylene treated rats (OX), and HFD + OX rats. **b** The effect of inhibition of NADPH oxidase with the Nox1/4 inhibitor GKT 137831 (0.3 μM) was assessed on NADPH (100 μM) O_2^- production. Results are expressed as counts per minute (cpm) per mg of tissue. Bars represented mean ± SEM of five animals. Statistical differences were calculated with ANOVA followed by Bonferroni as a *posterio* test and **a** $^{*}p<0.05$, $^{***}p<0.001$ versus basal levels; $^{\#}p<0.05$ OX, $^{\#\#\#}p<0.001$ versus HFD; **b** $^{*}p<0.05$, $^{**}p<0.01$, $^{***}p<0.001$ versus basal levels. $^{\dagger}p<0.05$, $^{\dagger\dagger}p<0.01$; $^{\dagger\dagger\dagger}p<0.001$ versus NADPH-stimulated

HFD, OX, and HFD + OX groups in vascular tissue (glomeruli), interstitium and tubules. These findings confirm that NADPH oxidase is a major source of ROS generation under pathological conditions such as diabetic nephropathy, CKD, [19, 20] and urolithiasis [18, 21]. Most importantly, we first identify NADPH oxidase isoform Nox1 as a main source of renal oxidative stress in hyperoxaluria and demonstrate a synergic effect on Nox-derived oxidative stress when obesity and hyperoxaluria converge. In contrast to Nox1, Nox4 was down-regulated in renal cortex from the different experimental groups, being lower as Nox-derived oxidative stress increased. Although some authors [21] have reported an up-regulation of Nox4 in hyperoxaluria, and this isoform has mostly been associated to oxidative stress in diabetic nephropathy and renal injury, recent studies of our group have demonstrated potential benefits of renal Nox4 on vasodilator function, performing a protective role in the Nox4 vasculature and being expressed both in renal vascular wall and in renal cortex [22].

Local inflammatory response and epithelial damage are key factors in the pathogenesis of stone formation. Once evaluated oxidative stress pathways, kidney local inflammatory responses involved in hyperoxaluria and under conditions of both hyperoxaluria and obesity were assessed to study the mechanism by which oxidative stress produces renal atrophy and loss of renal function. Expression of secondary mediators, such as NFκB1 and TNFα, chemoattractants as MCP-1, or crystallization modulators like OPN, was examined for this purpose. Interestingly, changes in expression of NFκB1, a redox-sensitive primary regulator involved in the host defense response were correlated with changes in oxidative stress levels and Nox1 expression, being significantly enhanced in OX and HFD + OX groups. NFκB1 pathways are activated in a variety of experimental models of renal inflammatory disease, including ethylene glycol-induced nephrolithiasis or ureteric obstruction [23]. Our results confirm an NFκB1 response parallel to the Nox1-derived oxidative stress response, triggered by hyperoxaluria and enhanced by HFD, thus showing the involvement of redox-sensitive transcription. Both HFD feeding and urolithiasis are known to increase TNF α expression and macrophage renal cortex infiltration [24, 25]. Furthermore, expression of the inflammatory mediator TNFα was also found to be significantly higher in the renal cortex of the OX and HFD + OX groups, but only moderate in the HFD group. Immunofluorescence showed TNFα expression mainly in renal tubules. Szeto et al. reported a fourfold increase in kidney TNFα expression in a HFD mouse model, in which HFD was administered during 24 weeks [25]. In our study, there was just a slight difference in TNFα RNAm levels between the HFD and the control group due to a shorter exposition to HFD (8 weeks), but TNFα gene expression markedly increased in OX rats fed a HFD thus suggesting

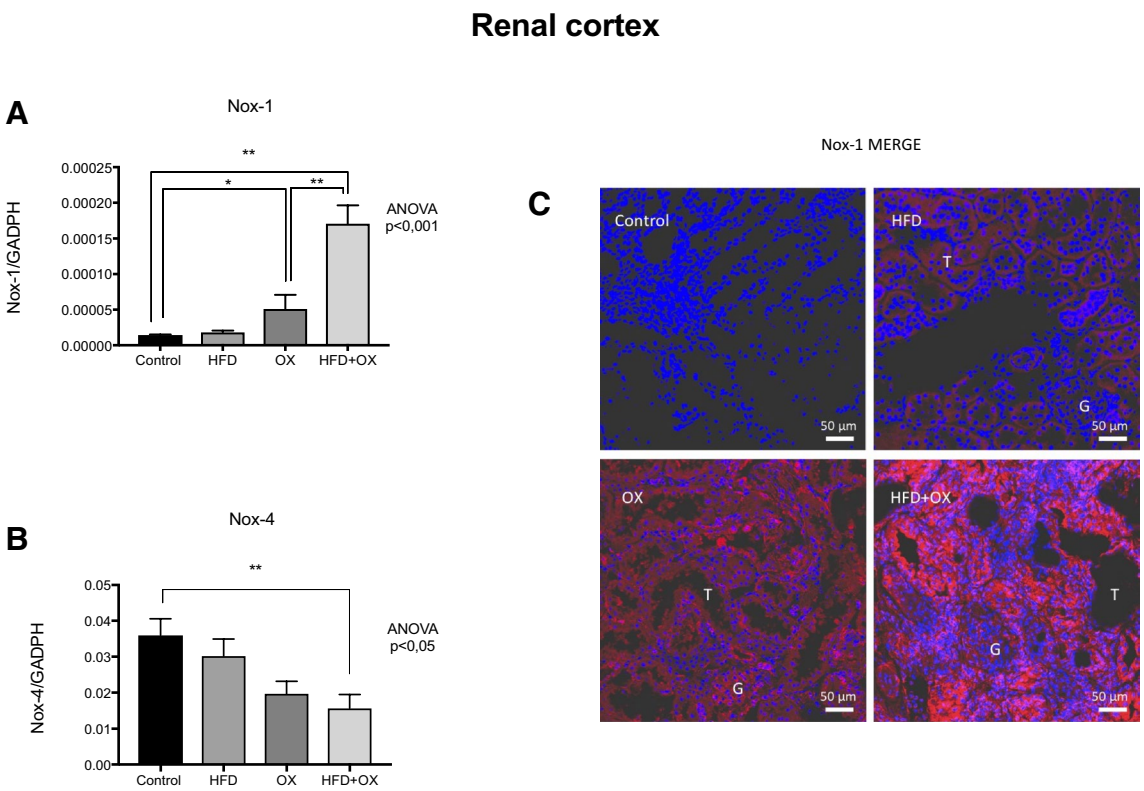

Fig. 6 Nox1 is higher expressed as renal damage is more severe both in glomeruli and in tubules from rat kidney. Conversely Nox4 expression is significantly lower when kidney damage is higher. **a**, **b** RT-PCR analysis of Nox1 (**a**) and Nox4 (**b**) expression in samples of renal cortex, showing that Nox1 was higher and Nox4 lower, OX and HFD + OX groups, respectively. Results were quantified by relative quantification of gene expression using Nox1 and Nox4 as the target genes, and GAPDH as reference gene. Results are presented as a ratio of Nox1 or Nox4 expression vs. GADPH from the sample. Data are shown as mean ± SEM of five animals. Significant differences were analyzed using unpaired *t* test $*p < 0.05$, $**p < 0.01$. ANOVA test was used for detecting differences between all groups. **b** Immunofluorescence demonstration of Nox1 in renal cortex from rat kidney. Immunofluorescence double labeling for TO-PRO marker (blue areas) demonstrates nuclear staining and for Nox1 protein (red areas), which was distributed throughout the cortex, both in tubules (T) and glomeruli (G). As RT-PCR, expression was higher in OX and HFD + OX groups, when renal damage was increasing. Control group did not show any expression. Scale bars indicate 50 µm. Sections are representative of $n = 3$ animals

an inflammatory response associated to pronounced Nox-1-derived oxidative stress and up-regulation of the NFκB1 pathway.

OPN, a potent inhibitor of crystallization of calcium phosphate, is enhanced in the kidney of rats with experimentally induced calcium nephrolithiasis [26] Proteomic analysis of human renal calculi has confirmed also an important role for the inflammatory processes in calcium stone formation, OPN being involved [27]. MCP-1 is a powerful and specific chemotactic factor for recruiting monocytes, macrophages, and lymphocytes. It is significantly overexpressed when tubular lumen crystals move to the renal interstitium, and has been suggested to be responsible for the leukocyte influx that leads to tubular inflammation and renal damage [28]. In our model, both OPN and MCP-1 were up-regulated in hyperoxaluric rats (OX and HFD + OX groups), being maximal in the HFD + OX group. Even though our model was a model of mild early obesity in young rats, and short to mimic a severe obesity, with altered lipid profile, the present results demonstrate its influence in triggering an oxidative stress status responsible of the worsening of renal function secondary to a higher crystal deposition, an inflammatory infiltration and a tubular atrophy, when concurs with hyperoxaluria. Not only oxidative stress metabolic pathways were severely disturbed, but also local inflammatory response and tubular damage were achieved. These

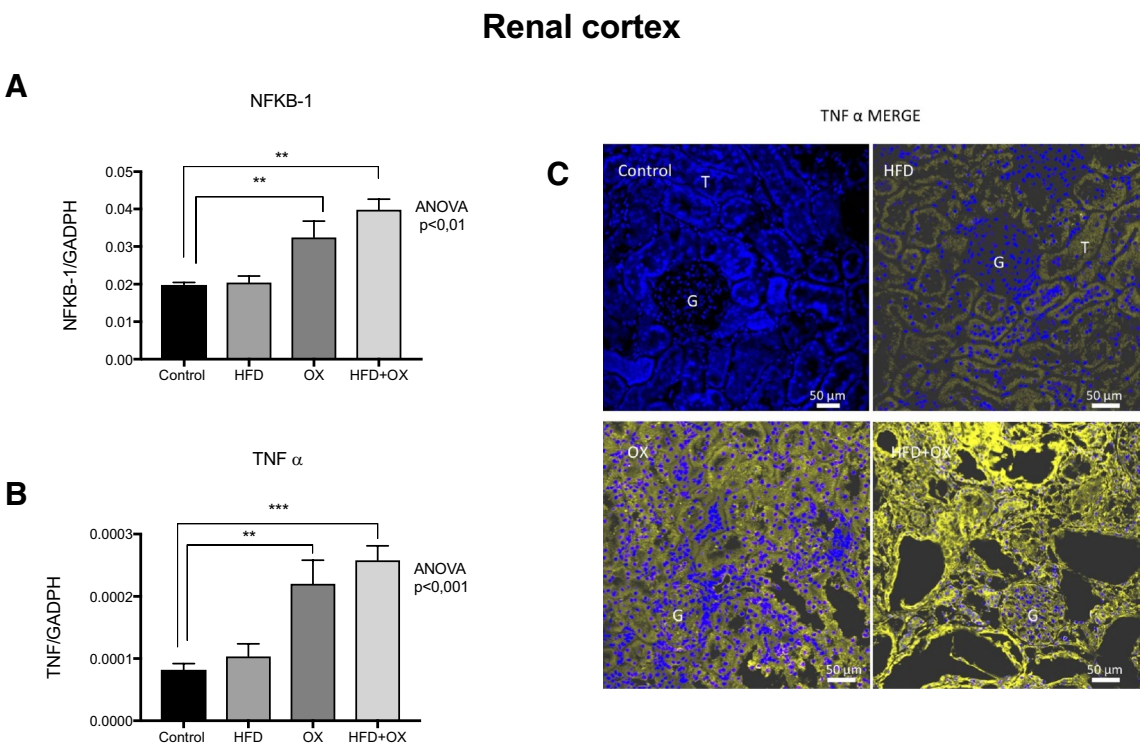

Fig. 7 NFκB1 and TNFα are higher expressed as renal damage is more severe both in glomeruli and in tubules from rat kidney. **a**, **b** RT-PCR analysis of NFκB1 (**a**) and TNFα (**b**), in samples of renal cortex showing that both genes were expressed higher in HFD, OX and HFD + OX groups. Results were quantified by relative quantification of gene expression using NFκB1 (**a**) and TNFα (**b**), as the target genes, and GAPDH as reference gene. Results are presented as a ratio of target expression vs. GADPH, from the sample. Data are shown as the mean ± SEM of five animals. Significant differences were analyzed using unpaired *t* test $*p < 0.05$, $**p < 0.01$. ANOVA test was used for detecting differences between all groups. **b** Immunohistochemical demonstration of TNFα in renal cortex from rat kidney. Immunofluorescence double labeling for TO-PRO marker (blue areas) demonstrates nuclear staining, and for TNF α (yellow areas), which was distributed throughout the cortex, initially in tubules (T), and when a higher expression was showed, in glomeruli (G). As RT-PCR TNF α expression, immunofluorescence showed slight expression in HFD, and more enhanced in OX and HFD + OX groups, when renal damage was increasing. Control group did not show any expression. *Scale bars* indicate 50 µm. Sections are representative of $n = 3$ animals

results enhance the importance of diet as an independent factor of nephrolithiasis-associated kidney injury.

Conclusions

In conclusion, the present study demonstrates that oxidative stress is a key pathogenic factor in renal disease associated with lithiasis, and a common link between lithiasis and obesity-related renal injury, which has additive effects in triggering an important kidney inflammatory response. COX-2 and xanthine oxidase pathways must be considered as metabolic pathways involved in the oxidative stress response and should be taken into account when designing new therapeutic approaches for the renal injury associated to lithiasis. Interestingly, the NADPH oxidase isoform Nox1 is first identified as a major source of oxidative stress in nephrolithiasis and responsible of the oxidative stress burst when lithiasis and obesity concur thus representing a new therapeutic target, in contrast to Nox4 which does not contribute to enhanced ROS generation. NF-KB and TNF α pathways blockade should also be investigated for urolithiasis treatment.

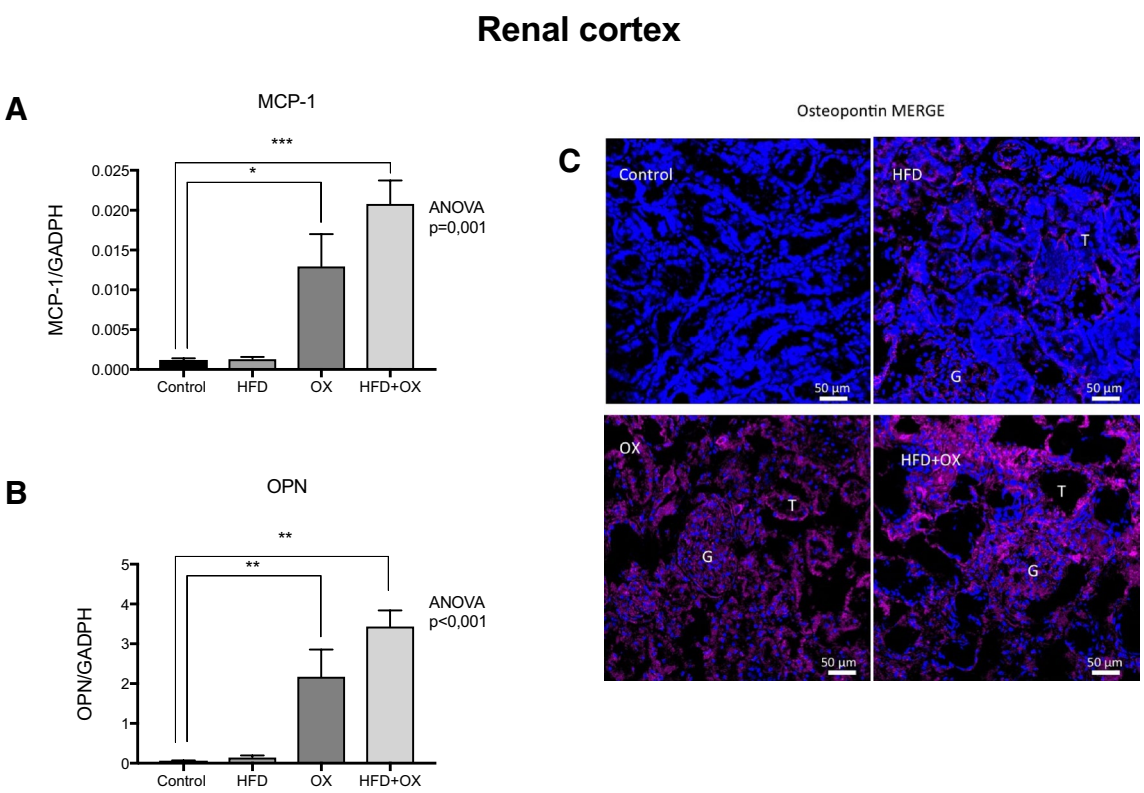

Fig. 8 MCP-1 and OPN are higher expressed as renal damage is more severe both in glomeruli and in tubules from rat kidney. **a**, **b** RT-PCR analysis of MCP-1 (**a**) and OPN (**b**) in samples of renal cortex, showing that MCP-1 and OPN were expressed higher in OX and HFD + OX groups. Results were quantified by relative quantification of gene expression using MCP-1 (**a**) and OPN (**b**), as the target genes, and GAPDH as reference gene. Results are presented as a ratio of target expression vs. GADPH, from the sample. Data are shown as mean ± SEM of five animals. Significant differences were analyzed using unpaired *t* test $*p<0.05$, $**p<0.01$, $***p<0.001$. ANOVA test was used for detecting differences between all groups. **b** Immunohistochemical demonstration of OPN in renal cortex from rat kidney. Immunofluorescence double labeling for TO-PRO marker (blue areas) demonstrates nuclear staining, and for OPN (fuchsia areas), which was distributed throughout the cortex, predominantly in tubules (T), but also in glomeruli (G), and interstitium. As RT-PCR OPN alpha´s expression, immunofluorescence showed higher expression in OX and HFD + OX groups, when renal damage was increasing. Interestingly HFD group showed a slight expression. Control group did not show any expression. Scale bars indicate 50 µm. Sections are representative of $n=3$ animals

Funding Spanish Urological Foundation. The Spanish Urological Association funded this study. AEU Research Grant 2017 and Grant SAF2016-77526-R from the Spanish Ministry of Economy and Competitivity.

Data availability statement The datasets generated during and/or analyzed during the current study are available from the corresponding author on reasonable request.

Compliance with ethical standards

Conflict of interest The authors declare that they have no conflict of interest.

References

1. Scales CD, Smith AC, Hanley JM, Saigal CS, Urologic DIAP (2012) Prevalence of kidney stones in the United States. Eur Urol 62:160–165
2. Tungsanga K, Sriboonlue P, Futrakul P, Yachantha C, Tosukhowong P (2005) Renal tubular cell damage and oxidative stress in renal stone patients and the effect of potassium citrate treatment. Urol Res 33:65–69
3. Touyz RM, Briones AM, Sedeek M, Burger D, Montezano AC (2011) Nox isoforms and reactive oxygen species in vascular health. Mol Interv 11:27–35
4. Zuo J, Khan A, Glenton PA, Khan SR (2011) Effect of NADPH oxidase inhibition on the expression of kidney injury molecule and calcium oxalate crystal deposition in hydroxy-L-proline-induced hyperoxaluria in the male Sprague–Dawley rats. Nephrol Dial Transpl 26:1785–1796
5. Joshi S, Peck AB, Khan SR (2013) NADPH oxidase as a therapeutic target for oxalate induced injury in kidneys. Oxid Med Cell Longev 2013:462361
6. Wang Y, Chen X, Song Y, Caballero B, Cheskin LJ (2008) Association between obesity and kidney disease: a systematic review and meta-analysis. Kidney Int 73:19–33
7. Jonassen JA, Kohjimoto Y, Scheid CR, Schmidt M (2005) Oxalate toxicity in renal cells. Urol Res 33:329–339

8. Joshi S, Wang W, Peck AB, Khan SR (2015) Activation of the NLRP3 inflammasome in association with calcium oxalate crystal induced reactive oxygen species in kidneys. J Urol 193:1684–1691
9. Sáenz-Medina J, Jorge E, Corbacho C, Santos M, Sánchez A, Soblechero P et al (2018) Metabolic syndrome contributes to renal injury mediated by hyperoxaluria in a murine model of nephrolithiasis. Urolithiasis 46:179–186
10. Muñoz M, López-Oliva ME, Pinilla E et al (2017) CYP epoxygenase-derived H. Free Radic Biol Med 106:168–183
11. Khan SR (2005) Hyperoxaluria-induced oxidative stress and antioxidants for renal protection. Urol Res 33:349–357
12. Ebenezer PJ, Mariappan N, Elks CM, Haque M, Francis J (2009) Diet-induced renal changes in Zucker rats are ameliorated by the superoxide dismutase mimetic TEMPOL. Obesity (Silver Spring) 17:1994–2002
13. Munoz M, Sanchez A, Pilar Martinez M et al (2015) COX-2 is involved in vascular oxidative stress and endothelial dysfunction of renal interlobar arteries from obese Zucker rats. Free Radic Biol Med 84:77–90
14. Elmarakby AA, Imig JD (2010) Obesity is the major contributor to vascular dysfunction and inflammation in high-fat diet hypertensive rats. Clin Sci (Lond) 118:291–301
15. Wong WT, Wong SL, Tian XY, Huang Y (2010) Endothelial dysfunction: the common consequence in diabetes and hypertension. J Cardiovasc Pharmacol 55:300–307
16. Feig DI, Kang DH, Johnson RJ (2008) Uric acid and cardiovascular risk. N Engl J Med 359:1811–1821
17. Eleftheriadis T, Pissas G, Antoniadi G, Liakopoulos V, Stefanidis I (2018) Allopurinol protects human glomerular endothelial cells from high glucose-induced reactive oxygen species generation, p53 overexpression and endothelial dysfunction. Int Urol Nephrol 50:179–186
18. Khan SR, Joshi S, Wang W, Peck AB (2014) Regulation of macromolecular modulators of urinary stone formation by reactive oxygen species: transcriptional study in an animal model of hyperoxaluria. Am J Physiol Renal Physiol 306:F1285–F1295
19. Sedeek M, Nasrallah R, Touyz RM, Hébert RL (2013) NADPH oxidases, reactive oxygen species, and the kidney: friend and foe. J Am Soc Nephrol 24:1512–1518
20. Ratliff BB, Abdulmahdi W, Pawar R, Wolin MS (2016) Oxidant mechanisms in renal injury and disease. Antioxid Redox Signal 25:119–146
21. Sharma M, Sud A, Kaur T, Tandon C, Singla SK (2016) *N*-acetylcysteine with apocynin prevents hyperoxaluria-induced mitochondrial protein perturbations in nephrolithiasis. Free Radic Res 50:1032–1044
22. Muñoz M, Martínez MP, López-Oliva ME et al (2018) Hydrogen peroxide derived from NADPH oxidase 4- and 2 contributes to the endothelium-dependent vasodilatation of intrarenal arteries. Redox Biol 19:92–104
23. Chuang YH, Chuang WL, Huang SP, Liu CK, Huang CH (2009) Inhibition of nuclear factor-kappa B (NF-kappaB) activation attenuates ureteric damage in obstructive uropathy. Pharmacol Res 60:347–357
24. Taguchi K, Okada A, Hamamoto S et al (2015) Proinflammatory and metabolic changes facilitate renal crystal deposition in an obese mouse model of metabolic syndrome. J Urol 194:1787–1796
25. Szeto HH, Liu S, Soong Y, Alam N, Prusky GT, Seshan SV (2016) Protection of mitochondria prevents high-fat diet-induced glomerulopathy and proximal tubular injury. Kidney Int 90:997–1011
26. Khan SR, Johnson JM, Peck AB, Cornelius JG, Glenton PA (2002) Expression of osteopontin in rat kidneys: induction during ethylene glycol induced calcium oxalate nephrolithiasis. J Urol 168:1173–1181
27. Merchant ML, Cummins TD, Wilkey DW et al (2008) Proteomic analysis of renal calculi indicates an important role for inflammatory processes in calcium stone formation. Am J Physiol Renal Physiol 295:F1254–F1258
28. Boonla C, Hunapathed C, Bovornpadungkitti S et al (2008) Messenger RNA expression of monocyte chemoattractant protein-1 and interleukin-6 in stone-containing kidneys. BJU Int 101:1170–1177